Journal of
Ceramic Science
and Technology

*J. Ceram. Sci. Tech.*, **05** [04] 293-298 (2014)
DOI: 10.4416/JCST2014-00019
available online at: http://www.ceramic-science.com


# Preparation and Characterization of Hydroxyapatite/Alumina Nanocomposites by High-Energy Vibratory Ball Milling

**A. E. Hannora***

Suez University, Faculty of Petroleum and Mining
Engineering, Department of Science and Mathematics, Suez, Egypt, 43721.
received May 14, 2014; received in revised form July 3, 2014; accepted August 13, 2014

**Abstract**

**Hydroxyapatite/alpha-alumina composites were prepared by means of high-energy vibratory ball milling. The effect of the addition of alumina, from 5 to 25 wt%, was investigated. x-ray diffraction (XRD) and Fourier transform infrared spectroscopy (FT-IR) results indicated that hydroxyapatite and alumina were the major phases after mechanical milling and only small peak shifts were observed. Transmission electron microscope (TEM) photomicrographs revealed that the powder obtained after mechanical milling was composed of nanoparticles in the size of ~ 40 nm. After 3h of air sintering at 1000 – 1200 °C, beta-tricalcium phosphate and alumina phases were found. The additional calcium aluminum phosphate phase might be formed during the sintering process at 1200 °C. The mechanical properties (compressive strength and Rockwell hardness) of the hydroxyapatite/alumina composites were improved with sintering temperatures and concentrations of alumina and the maximum value was found with 15 wt % alumina.**

*Keywords: Mechanical alloying, hydroxyapatite, alumina and nanocomposite materials.*

## I. Introduction

Calcium phosphate (CaP) materials are currently used for bone substitutes in many different clinical applications. Different types of CaP such as hydroxyapatite (HA), tetra calcium phosphate (TTCP), tricalcium phosphate (TCP), dicalcium phosphate anhydrous (DCP), amorphous calcium phosphate (ACP) and biphasic calcium phosphate (BCP) are available for use as hard tissue substitute [1]. Hydroxyapatite ($Ca_{10}(PO_4)_6(OH)_2$) is the most promising material for bone replacement thanks to its osteoconductivity and bio-compatibility properties. However, the application of HA is limited to low-stress regions owing to its relatively low mechanical properties and high dissolution rate [2–4]. HA is similar to the inorganic part of the bone matrix and is stable in body fluid while TCP tends to be soluble and is used as bio-cement or bone filler [5].

Ceramic oxides or metallic dispersions have been introduced as reinforcing agents [6]. Among the ceramic reinforcements, alumina ceramics have been used for orthopaedic surgery as hip prostheses and in dentistry as dental implants. Their widespread use is based on a combination of good strength, modest fracture toughness, high wear resistance, good biocompatibility and excellent corrosion resistance. Alumina has also been used in jaw bone reconstruction. Other clinical applications of alumina include knee prostheses, bone segment replacements, bone screws, middle ear bone substitutes, and corneal replacements [7–9].

Alumina powder has been added to HA powder in order to obtain high fracture toughness. Alumina has good mechanical properties compared with HA, and exhibits extremely high stability with human tissues [10]. Bioceramics are classified mainly into three groups on the basis of the interactions between the implant material and the tissues. These groups are termed bioinert, bioactive and bio-resorbable bioceramics respectively. Alumina is a bioinert ceramic while hydroxyapatite is a bioactive ceramic and tricalcium phosphate a bio-resorbable ceramic [11].

Nanocomposites have received a great deal of attention owing to their superior mechanical properties in comparison with their large-grained counterparts. Nanocrystalline alumina is bioactive whereas alumina is bioinert in conventional polycrystalline form [12]. For HA/alumina composites, α-alumina powder was used because of its better sinterability than γ-alumina [13].

Mechanical alloying (MA) is a potential method for the preparation of various interesting solid-state materials and takes advantage of the perturbation of surface-bonded species by pressure to enhance thermodynamic and kinetic reactions between solids. Over the past decades, MA has been widely developed for the fabrication of a wide range of advanced materials such as intermetallics, nanocrystalline alloys or ceramic materials [14]. Mechanical alloying/milling is a solid-state powder processing technique involving cold-welding and fracturing of powder particles. The constituent powder particles are repeatedly fractured and cold-welded, so that powder particles with very fine structure can be obtained after milling [15]. The effect of high-energy ball milling (HEBM) on hydroxyapatite with titanium and silicon has recently been described. During HEBM process, the impacts of the milling balls result in a significant decrease of the HA particle and crystalline size, forming the nano-scale structure [16, 17].

* Corresponding author: Ahmed.Hannora@suezuniv.edu.eg

The purpose of the present study is to produce HA/alumina composite by means of the vibratory ball milling technique. The effect of alumina additive on microstructure of HA is investigated by means of transmission electron microscopy (TEM). x-ray diffraction analysis (XRD) and Fourier transform infrared spectroscopy (FT-IR). Also, the influence of the HA/alumina system decomposition on the mechanical properties after sintering in air atmosphere is employed.

## II. Materials and Samples

Alpha alumina and hydroxyapatite-powder (Sigma-Aldrich No. 21223) were placed into 20-cm$^3$ high-energy vibratory ball milling vials (50 Hz) for one hour, with hard steel balls. The powders were treated with the optimum ball to powder ratio, equal to 20:1. As-prepared samples were pressed under isostatic pressure of 100 bar with a diameter of ~ 5 mm and a height of ~ 8 mm, in order to obtain a suitable specimen for heat treatment at 1000 and 1200 °C for 3 h. The heating time was measured from the point at which the furnace reaches the heating temperature. All the sintered samples were furnace-cooled.

XRD was performed with a Siemens D5000 powder diffractometer using Cu $K_\alpha$ radiation (wavelength $\lambda$ = 0.15406 nm) with a nickel filter at 40 KV and 30 mA. The diffractometer was operated within the range of $20° < 2\theta < 60°$ with step-time = 3 seconds and step-size = 0.01 degrees. Diffraction signal intensity throughout the scan was monitored and processed with DIFFRACplus software. Microstructural features of the mechanically treated powder have been systematically investigated using JEOL TEM-2100. Spectra from 4000 to 400 cm$^{-1}$ were recorded by means of Bruker TENSOR 27 FT-IR spectrometers, 2 cm$^{-1}$ resolution.

Thermal characterization was performed in the temperature range from 25 to 1000 °C using a Shimadzu Differential Thermal Analyzer DTA 50, heating rate 10 K/min. Heat-treated compacted samples were loaded under compression until failure using a INSTRON Universal Testing Machine (4208) at a cross-head speed of 0.016 mm/min from where the compressive strength was measured. Surface hardness was tested with a Rockwell Hardness Tester HRA-scale.

## III. Results and Discussion

The function of HA in all its applications is largely determined by its morphology, composition, crystal structure, and crystal size distribution. Thus, to control the mechanical properties of hydroxyapatite, the influence of synthesis conditions on such characteristics as particle morphology and size distribution, as well as agglomeration have to be studied [18]. The XRD patterns shown in Fig. 1 illustrate the effect of mechanical treatment on the HA and α-alumina powder. After one hour of high-energy ball milling, the HA peaks show a notable intensity reduction as a result of severe plastic deformation. Owing to the alpha-alumina structural stability, the intensities of its diffraction pattern get stronger with increasing alumina content. No additional phases were detected in these composite samples except a small shift of the XRD patterns to a lower angle with mechanical milling owing to accumulated strain.

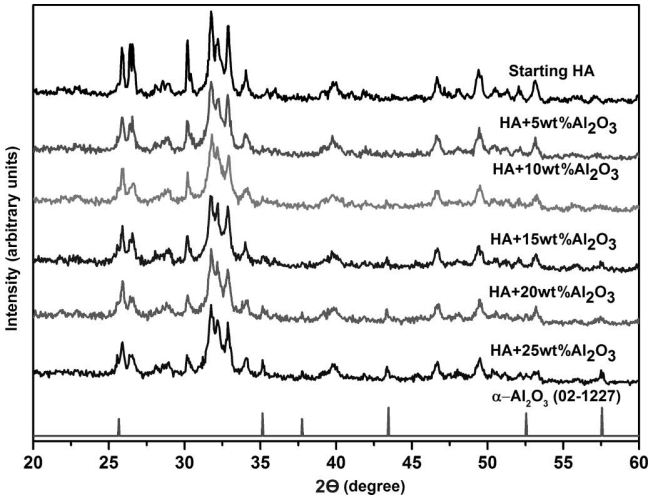


**Fig. 1:** XRD patterns of high-energy mechanically treated HA with alumina addition after 1h.

Transmission electron microscopy (TEM) was used to analyze the morphology of the treated powders after high-energy ball milling. Figs. 2 (a) and (b), respectively, confirming that the grain size of the as-milled samples is in the order of tens of nanometers (less than 50 nm). The morphologies of the HA powder particles before and after ball milling were studied in our preceding work [17]. As mentioned before, cold welding and fracturing are the two essential processes involved in the HEBM process. Fracture tends to break individual particles into smaller pieces and deagglomerates particles that have been cold-welded. The morphology of the initial large particles significantly changes owing to fracture, agglomeration, and deagglomeration processes. After one hour of mechanical milling, rod and irregular shape morphologies were found. Also, it can be seen that these small particles formed the agglomerates as a result of a cold-welding phenomenon during ball milling.

The FT-IR spectra of mechanically milled HA, and HA/alumina powder are shown in Fig. 3. For all the specimens, the vibration bands showed typical apatite characteristics, with phosphate group bands at around 469 ($\nu_2$), 559 ($\nu_4$), 601 ($\nu_4$), 961 ($\nu_1$), 1020 ($\nu_3$), and 1097 ($\nu_3$) cm$^{-1}$. The broad peak at 867 cm$^{-1}$ band was the characteristic peak of hydrogen phosphate group. The broad absorption band around 634 belongs to –OH, which is in good agreement with results suggested by several authors [1, 9]. The increasing alumina addition enhances the 469 ($\nu_2$) band while the sharpness of the other bands decreases. The broadening and slight shift of the FT-IR spectra found with alumina addition could be due to both severe plastic deformation as a result of the milling process and/or interaction of HA with the addition of alumina, which is known to have very hard particles. It was also found that no new peaks appeared with the addition of alumina. The FT-IR result combined with the x-ray diffraction indicated that separate phases of hydroxyapatite and alumina without interaction were found after one hour of the HEBM process.

Sintering temperature is an important factor, which adversely affects the strength of HA. For instance, sintering at elevated temperatures has a tendency to eliminate

the functional group OH in the HA matrix (dehydration) and results in the decomposition of HA into α-tricalcium phosphate (α-TCP), β-tricalcium phosphate (β-TCP) and tetracalcium phosphate (TTCP) [18,19]. It is reported that at sintering temperatures from 650 to 1200 °C, HA decomposes into β-tricalcium phosphate [18] while at the sintering temperature at 1200 °C and higher, α-tricalcium phosphate and tetracalcium phosphate were formed [10]. In order to assess the influence of heat treatment, the samples were characterized with x-ray diffraction. The XRD patterns of the compacted HA powder after heat treatment at 1000 and 1200 °C for three hours are shown in Figs. 4 and 5. The HA has completely disappeared and the exactly formed phase was matched with ICDD (JCPDS) standard for β-TCP and calcium aluminum phosphate. It is reported that HA is similar to the inorganic part of the bone matrix and is stable in body fluid while TCP is rather soluble and is used as bio-cement or bone filler. These ceramics are used in porous, granular, and dense forms [5].

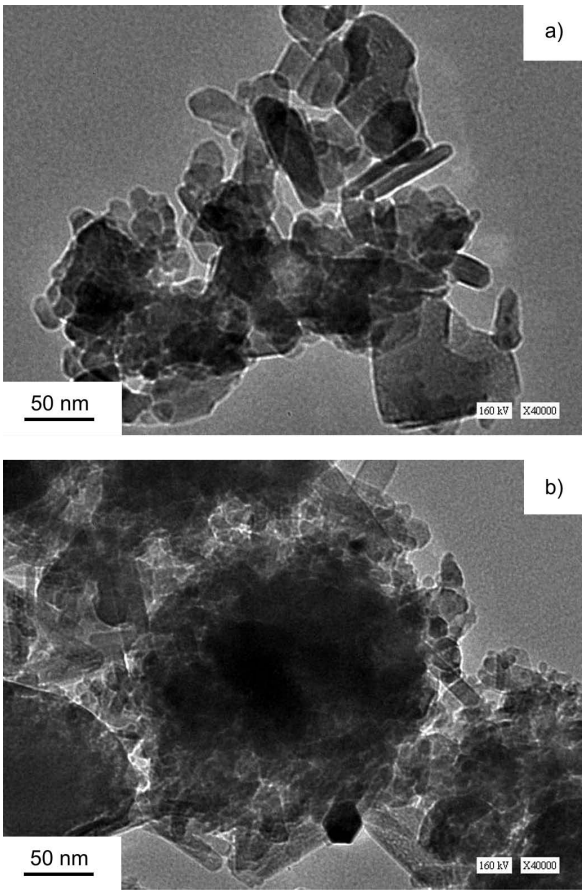


**Fig. 2:** Bright field image of hydroxyapatite with (a) 10 wt% and (b) 15 wt% alumina after one hour of mechanical treatment.

At sintering temperatures of 1000 °C, Fig. 4, the addition of alumina content (up to 15 wt%) partially reacted with hydroxyapatite, there is no evident trace of alumina in the XRD patterns, and the formed phase exactly matched to the β-TCP. The same phase, β-TCP, was found with higher alumina content (more than 15 wt%) as well as extra peaks related to the alumina phase. Fig. 5 also shows the heat treatment at higher temperature, 1200 °C, which confirms the formation of β-TCP in addition to the alumina. The calcium aluminum phosphate phase $Ca_9Al(PO_4)_7$ was also formed for all alumina contents at this temperature. It is reported that formation of calcium aluminate phases has been observed during the solid-state reaction between hydroxyapatite and alumina owing to the reaction between Ca and alumina. The calcium aluminates phases formed were related to HA transformation to β and α-TCP [2,20]. MA has been shown to be capable of synthesizing a variety of equilibrium and non-equilibrium alloy phases starting from blended elemental or prealloyed powders [15]. The effect of high-energy mechanical milling could affect the HA/alumina powder resulting calcium aluminum phosphate phase formation. Fig. 6 shows a TEM image of sinteried HA with 15 wt% alumina at 1200 °C. The diffraction pattern shows the presence of extra spots which could relate to the unreacted alumina particles.

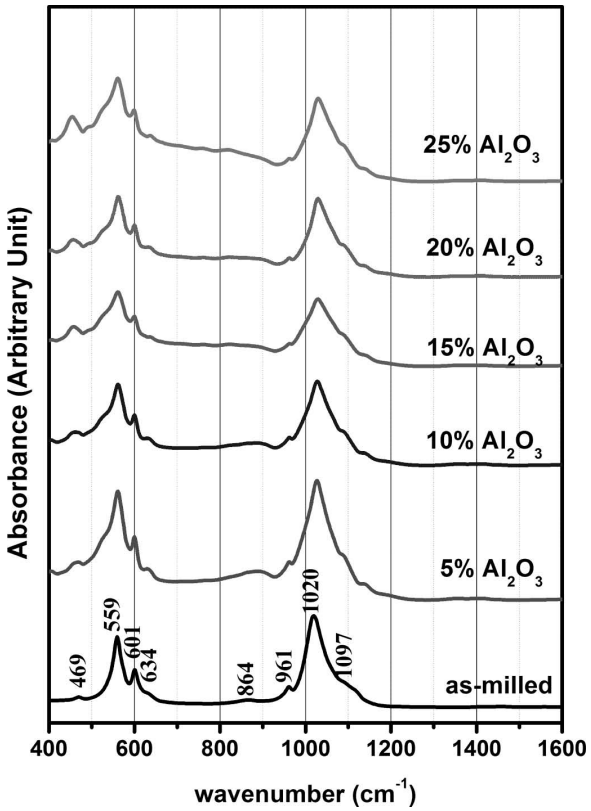


**Fig. 3:** FT-IR spectra of high energy mechanically treated hydroxyapatite/alumina.

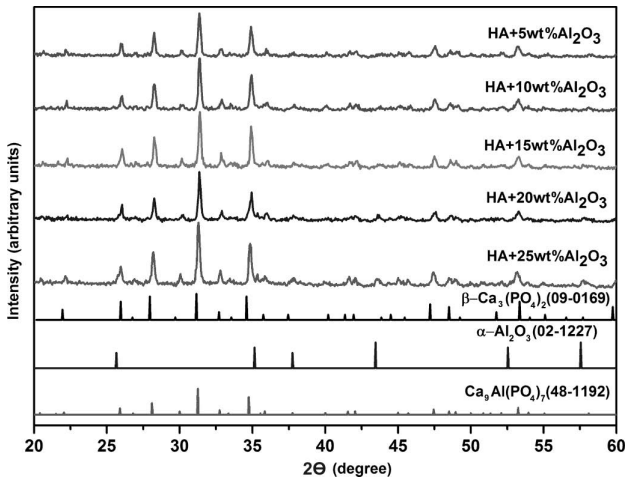


**Fig. 4:** XRD patterns of hydroxyapatite/alumina after sintering at 1000 °C for three hours.

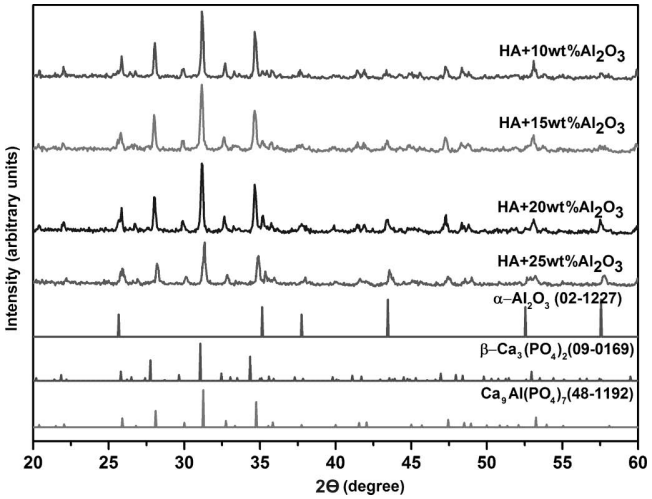


**Fig. 5:** XRD patterns of hydroxyapatite/alumina after sintering at 1200 °C for three hours.

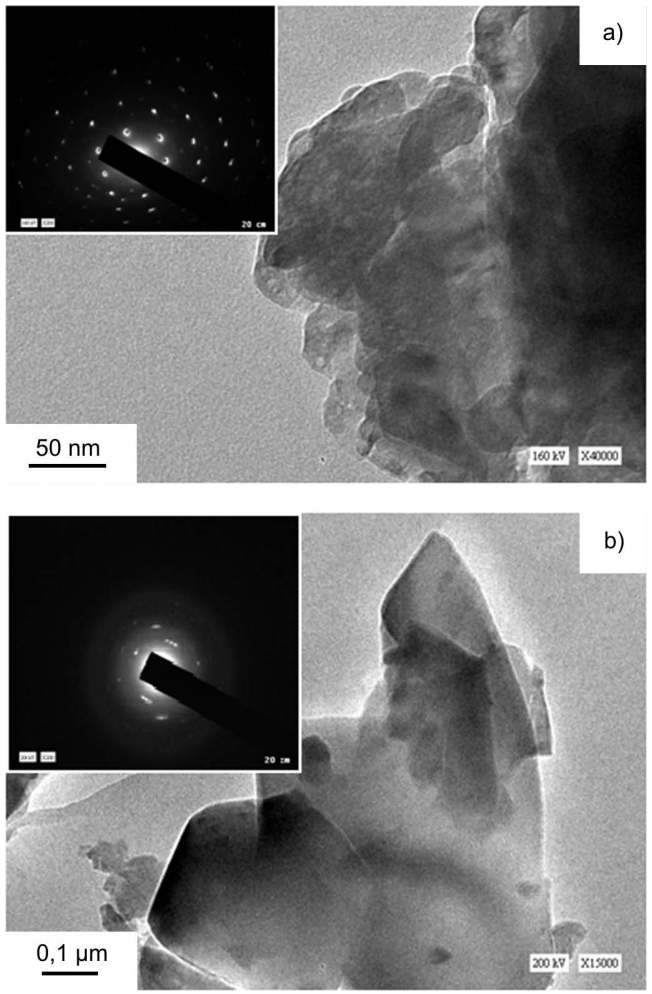


**Fig. 6:** TEM images with 15 wt% alumina addition after sintering at 1200 °C for three hours and electron diffraction pattern of an ordered phase.

The mechanical properties are governed not only by the amount of alumina addition but also by heat treatment conditions. It is reported that if the reinforcing agent such as alumina and zirconia is added to HA, the mechanical properties are reduced owing to the phase decomposition from HA to TCP. Also, when HA is reinforced with 20 wt% alumina and sintered at 1200 and 1300 °C, the samples were very brittle and friable [2,20]. It is worth mentioning that the decomposition of HA suppresses densification and is accompanied by a decrease in mechanical properties [18]. It is also reported that for the mechanical strength of the composites, HA mixed with 10 % $Al_2O_3$ exhibits the highest compressive strength with 813 MPa compared with 440 MPa for pure hydroxyapatite sintered at 1400 °C [21].

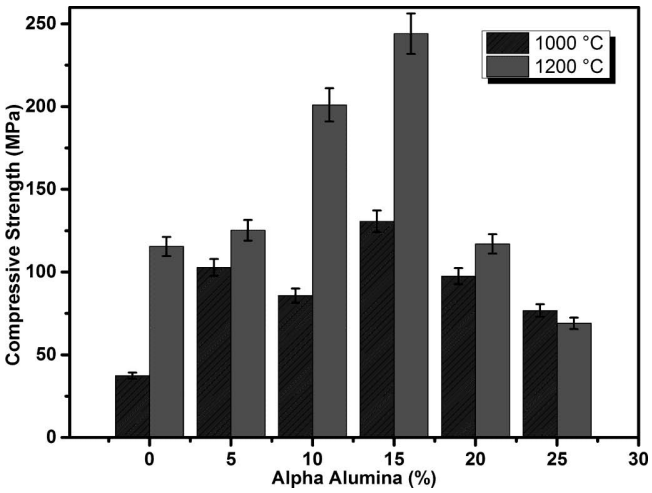


**Fig. 7:** Variation of compressive strength with alumina addition after sintering for three hours.

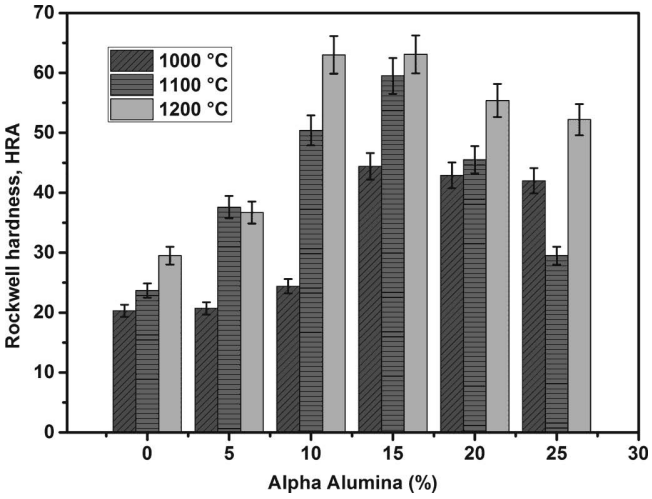


**Fig. 8:** Mean Rockwell hardness variations with alumina addition after 3h of sintering.

As shown in Figs. 7 and 8 significant increases in the compressive strength as well as Rockwell hardness with alumina addition at sintering temperatures (1000 – 1200 °C) are observed and reach the maximum value with 15 wt% then decreases. The compressive strength is shown to increase gradually with the addition of alumina and a maximum strength of 244 MPa is reached at 15 wt%. The improvement of the mechanical strength with alumina addition up to (15 wt%) could be due to the subsequent transformation of HA/alumina to calcium aluminum phosphate $Ca_9Al(PO_4)_7$. However, excess alumina in the composition could result in the formation of weakly bound alumina and calcium alumina phosphate phase and subsequently reduce the mechanical properties of high-alumina content. It is well known that reduction of the particle size contributes to the material strength and since a reduction

in particle size is observed, with mechanical milling this could play a significant role in increasing the mechanical properties.

## IV. Conclusion

- Hydroxyapatite/alumina nanocomposite can be successfully produced by means of high-energy vibratory ball milling from starting materials.
- The mechanical study (compression) highlights the positive effect of alumina addition on the mechanical properties after consolidation.
- Specimen containing 15 wt% alumina shows the maximum value for compressive strength and Rockwell hardness, so it can be used for direct compression owing to its satisfying flow and mechanical properties.
- Calcium aluminum phosphate $Ca_9Al(PO_4)_7$ phase was formed after heat treatment at 1200 °C of all samples.

## References


1 Rabiee, S.M., Moztarzadeh, F., Solati-Hashjin, M.: Synthesis and characterization of hydroxyapatite cement, *J. Mol. Struct.*, **969**, 172 – 175, (2010).

2 Kim, S.-J., Bang, H.-G., Song, J.-H., Park, S.-Y.:. Effect of fluoride additive on the mechanical properties of hydroxyapatite/alumina composites, *Ceram. Int.*, **35**, 1647 – 1650, (2009).

3 Mobasherpour, I., Solati Hashjin, M., Razavi Toosi, S.S., Darvishi Kamachali, R.: Effect of the addition $ZrO_2$-$Al_2O_3$ on nanocrystalline hydroxyapatite bending strength and fracture toughness, *Ceram. Int.*, **35**, 1569 – 1574, (2009).

4 Wu, Z., He, L., Chen, Z.: Composite biocoating of hydroxyapatite/$Al_2O_3$ on titanium formed by al anodization and electrodeposition, *Mater. Lett.*, **61**, 2952 – 2955, (2007).

5 Jun, Y.-K., Kim, W.-H., Kweon, O.-K., Hong, S.-H..: The fabrication and biochemical evaluation of alumina reinforced calcium phosphate porous implants, *Biomaterials*, **24**, 3731 – 3739, (2003).

6 Ayed, F.B., Bouaziz, J.: Sintering of tricalcium phosphate-fluorapatite composites by addition of alumina, *Ceram. Int.*, **34**, 1885 – 1892, (2008).

7 Kim, C.Y., Jee, S.S.: Hydroxyapatite formation on bioactive-glazed alumina, *J. Eur. Ceram. Soc.*, **23**, 1803 – 1811, (2003).

8 Chakraborty, J., Chatterjee, S., Sinha, M.K., Basu, D.: Effect of albumin on the growth characteristics of hydroxyapatite coatings on alumina substrates, *J. Am. Ceram. Soc.*, **90**, 3360 – 3363, (2007).

9 Chakraborty, J., Chatterjee, S., Sinha, M.K., Basu, D.: Effect of albumin on the growth characteristics of hydroxyapatite coatings on alumina substrates, *J. Am. Ceram. Soc.*, **90**, 3360 – 3363, (2007).

10 Chiba, A., Kimura, S., Raghukandan, K., Morizono, Y.: Effect of alumina addition on hydroxyapatite biocomposites fabricated by underwater-shock compaction, *Mat. Sci. Eng. A*, **A350**, 179/183, (2003).

11 Yelten, A., Yilmaz, S., Oktar, F.N.: Sol-gel derived alumina-hydroxyapatite-tricalcium phosphate porous composite powders, *Ceram. Int.*, **38**, 2659 – 2665, (2012).

12 Viswanath, B., Ravishankar, N.: Interfacial reactions in hydroxyapatite/alumina nanocomposites, *Scripta Mater.*, **55**, 863 – 866, (2006).

13 Evis, Z., Doremus, R.: Coatings of hydroxyapatite — nanosize alpha alumina composites on Ti-6Al-4V, *Mater. Lett.*, **59**, 3824 – 3827, (2005).

14 Fathi, M.H., Mohammadi Zahrani, E.: Fabrication and characterization of fluoridated hydroxyapatitenanopowders via mechanical alloying, *J. Alloy. Compd.*, **475**, 408 – 414, (2009).

15 Suryanarayana, C.: Mechanical alloying and milling, *Prog. Mater. Sci.*, **46**, [1 – 2], 1 – 184, (2001).

16 Hannora, A., Mamaeva, A.,Mansurov, Z.: X-ray investigation of Ti-doped hydroxyapatite coating by mechanical alloying, *Surf. Rev. Lett.*, **16**, [5], 781 – 786, (2009).

17 Hannora, A.E., Mukasyan, A.S., Mansurov, Z.A.: Nanocrystalline Hydroxyapatite/Si coating by mechanical alloying technique, *Bioinorg. Chem. Appl.*, 390104, (2012).

18 Shih, W.J., Wang, J.W., Wang, M.C., Hon, M.H.: A study on the phase transformation of the nanosized hydroxyapatite synthesized by hydrolysis using in situ high temperature x-ray diffraction, *Mater. Sci. Eng. C*, **26**, [8], 1434 – 1438, (2006).

19 Ebadzadeh, T., Behnamghader, A., Nemati, R.: Preparation of porous hydroxyapatite ceramics containing mullite by reaction sintering of clay, alumina and hydroxyapatite, *Ceram. Int.*, **37,** 2887 – 2889, (2011).

20 Ji, H., Marquis, P.M.: Sintering behaviour of hydroxyapatite reinforced with 20 wt% $Al_2O_3$, *J. Mater. Sci.*, **28,** 1941 – 1945, (1993).

21 Juang, H.Y., Hon, M.H.: Fabrication and mechanical properties of hydroxyapatite-alumina composites, *Mater. Sci. Eng. C*, **2.1 – 2,** 77 – 81, (1994).